

## 유기실리콘화합물의 플라즈마 중합에 관한 연구 : 2. 플라즈마 중합막의 물성

박수영 · 김낙중 · 김은영 · 홍성일\* · 히로유키 사사베\*\*

한국과학기술연구원 기능성고분자실 · \*서울대학교 섬유공학과

\*\*일본 이화학연구소 생체고분자물리연구실

(1991년 10월 2일 접수)

## Plasma Polymerization of Organosilicon Compounds : 2. Physical Properties of Plasma Polymer

Soo Young Park, Nakjoong Kim, Un Young Kim, Sung Il Hong\*, and Hiroyuki Sasabe\*\*

Functional Polymers Laboratory, Korea Institute of Science and Technology, Cheong-Ryang  
P. O. Box 131, Seoul 130-650, Korea

\*Department of Textile Engineering, Seoul National University, San 56-1, Shin-Lim Dong,  
Kwan-Ak Ku, Seoul 151-742, Korea

\*\*Biopolymer Physics Laboratory, The Institute of Physical and Chemical Research (RIKEN),  
Wako, Saitama 351-01, Japan

(Received October 2, 1991)

**요 약 :** 플라즈마 중합의 에너지 조건(W/Fm)에 따른 유기실리콘 플라즈마 중합막의 밀도, 표면자유 에너지, 굴절률, 내부응력, 열적특성, 및 전기전도성의 변화를 상세히 검토하였다. 플라즈마 중합막의 이러한 물성들은 모두 W/Fm 값의 조절에 의해 체계적이고 대폭적인 변화를 보였으며 이는 중합막의 화학구조적 변화특성과 일치하였다. 플라즈마 중합막의 이러한 물성변화는 플라즈마 중합의 활성화 성장기구에 의해 잘 설명되었다.

**Abstract :** The density, surface free energy, refractive index, internal stress, thermal properties, and electrical properties of organosilicon plasma polymers were investigated in terms of the input energy level(W/Fm) of plasma polymerization. It was found that such material properties were uniquely controlled by W/Fm and also were in good correlations with their chemical structures. The controlled properties of plasma polymer were interpreted with the activation growth mechanism of plasma polymerization.

### INTRODUCTION

Recently, plasma polymerized organic films are

attempted for numerous applications such as electronic or optical devices, separation membranes, protective coatings, and biomedical materials due

to their excellent thin film properties and processing merits of thin film formation.<sup>1,2</sup> Many reports on these topics have shown the unique and excellent properties of plasma polymerized films for many technological applications.<sup>1,2</sup> The most important example is the organosilicon plasma polymer that was subject to large research efforts in last years. In Part I of this study,<sup>3</sup> it was shown that the chemical structure of plasma polymer was controlled not only by the chemical nature of monomer but also by the input energy level W/Fm of plasma reaction. Especially, it was shown that the chemical structure of organosilicon plasma polymer could be controlled in the intermediate range that extends over the two entirely different categories of material, namely, from the polymer-like material at low W/Fm to the inorganic-like material at high W/Fm. Therefore, it is important to note that the physical properties of plasma polymer, especially, those for specific applications should be investigated carefully as the function of W/Fm. Up to now, such an important aspect was little accounted of by many authors who evaluated the performance only in terms of the chemical nature of monomer using the plasma polymers prepared at arbitrary reaction conditions.<sup>1</sup> Therefore, the main purpose of this study (Part II) is to demonstrate the systematic control of some important properties of plasma polymer by the input energy level of plasma reaction based on the structure-property correlation and mechanistic consideration of plasma polymerization process.

## EXPERIMENTAL

### Plasma Polymerization

The detailed description of the plasma reactor and the general procedure of plasma polymerization should be referred to the experimental section of Part I.<sup>3</sup> Three organosilicon compounds, tetramethylsilane (TMS), hexamethyldisilazane (HMD-SIZ), and hexamethyldisiloxane (HMDSIO) were used as the starting materials (monomers) of plasma polymerization.

### Density

Plasma polymers deposited on the lower electrode of plasma reactor were stripped or scraped by razor blade. The density of these plasma polymer film or powder was measured using density gradient columns (Techne, model DC-1): ethanol/carbon tetrachloride gradient column was used for the density range of 0.79~1.59 g/cm<sup>3</sup> and carbon tetrachloride/bromoform column was used for the density range of 1.60~2.89 g/cm<sup>3</sup>. The temperature of these gradient columns was maintained at 23±0.1°C and the density of plasma polymer was read from the equilibrium floating position.

### Surface Free Energy

Plasma polymer films (ca. 1,000 Å thick) were deposited on glass substrate (Corning #2 cover glass, 25 mm×25 mm). The contact angles of water and methyleneiodide sessile drops (carefully controlled within 0.6~0.8 μl volume) on the film surface were measured using Erma Contact anglemeter model G-I. All the contact angles were measured immediately after placing a sessile drop on the sample surface at room temperature. At least 8 readings from different drops were averaged for the reliable value of contact angle whose standard deviation was less than 2°. The dispersion and polar components of surface free energy were calculated from the measured contact angles according to the method developed by Owens and coworker.<sup>4</sup>

$$1 + \cos\theta = \frac{2}{\gamma_1} [(\gamma_s^d \gamma_1^d)^{1/2} + (\gamma_s^p \gamma_1^p)^{1/2}] \quad (1)$$

where,  $\theta$  is the measured contact angle,  $\gamma_1$  is the surface energy of test liquid ( $=\gamma_1^d + \gamma_1^p$ ),  $\gamma_1^d$  is the dispersion component of  $\gamma_1$ ,  $\gamma_1^p$  is the polar component of  $\gamma_1$ ,  $\gamma_s$  is surface energy of solid film ( $=\gamma_s^d + \gamma_s^p$ ),  $\gamma_s^d$  is the dispersion component of  $\gamma_s$ ,  $\gamma_s^p$  is the polar component of  $\gamma_s$ . Substituting the measured contact angles of water ( $\theta_w$ ) and methyleneiodide ( $\theta_i$ ) with the surface energy values of respective test liquid ( $\gamma_1, \gamma_1^d, \gamma_1^p$ ; shown in Table 1) into eq 1 yielded two simultaneous equations which were solved for  $\gamma_s^d$  and  $\gamma_s^p$  of plasma poly-

mer.

### Refractive Index

The refractive index of plasma polymer was evaluated by Gaertner L117 manual ellipsometer using the samples prepared for the measurement of contact angles. He-Ne laser was used as the light source and an incidence angle of  $50^\circ$  was maintained for all the measurements. A computer program supplied by the manufacturer (GP2 and Sub P) was used for the calculation of refractive index.

### Internal Stress

The expansive internal stress retained in the plasma polymer film was measured according to the method developed by Yasuda and coworker.<sup>6</sup> Polyethylene strip (12 mm × 100 mm, 70 μm thickness,  $E = 10^9$  dynes/cm<sup>2</sup>) was positioned on the lower electrode of plasma reactor and fixed at both ends using aluminum adhesive tapes. After the deposition of plasma polymer, both ends were cut using a razor blade, and the equilibrium curling radius (R) of the sample was measured with a caliper at the next day. Then, the internal stress ( $\sigma_s$ ) of plasma polymer was calculated from eq 2.

$$\sigma_s = ED/6Rd \quad (2)$$

where, E is the Young's modulus of substrate film, D is the thickness of substrate film, R is the measured equilibrium radius, and d is the thickness of plasma polymer film.

### Thermal Properties

Thermal properties of plasma polymer stripped or scraped from the lower electrode of plasma reactor were investigated by the Thermogravimetry (TGA) or Differential Thermal Analysis (Perkin-Elmer TGS II, and Rigaku DT/TGA model 8150).

### Electrical Properties

The metal/plasma polymer/metal (MIM) sandwich structure was prepared for the measurement of dielectric constant (relative permittivity) and DC conductivity (Fig. 1). Capacitance and dissipation factor of the MIM cell were measured by LCR meter (Ando Type AG-4303) at 1 kHz frequency. Relative permittivity ( $\epsilon$ ) of plasma polymer was then

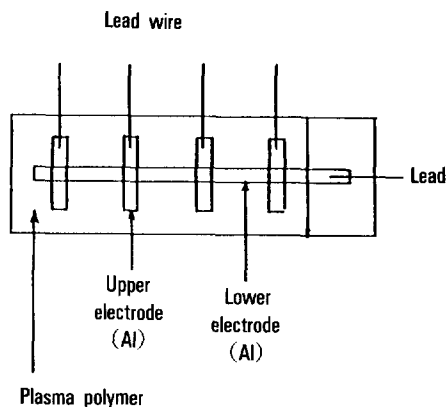


Fig. 1. Metal/plasma polymer/metal (MIM) sandwich cell for electrical property measurement.

calculated from eq 3.

$$\epsilon = d C_p / \epsilon_0 A \quad (3)$$

where, d is the thickness of plasma polymer,  $C_p$  is the parallel capacitance,  $\epsilon_0$  is the dielectric constant of vacuum, and A is the effective electrode area ( $2.4 \times 2.4$  mm<sup>2</sup>). Current-voltage characteristics of the MIM cell were measured using the DC power supply (0~100 Volts variable, Hyupseung Electronics), digital multimeter (Advantest TR 68 45) and digital electrometer (Keithley 616).

## RESULTS AND DISCUSSION

In Part I of this study,<sup>3</sup> it was shown that the chemical structure of plasma polymer was largely controlled by W/Fm over the full range of chemical structure which locates somewhere between the polymeric and inorganic materials. Generally, polymeric material is soft and flexible due to the one dimensional long-chain nature of chemical bonds, on the other hand, inorganic material is extremely dense and tough due to the three dimensional tight network of covalent bonds. Since the plasma polymers are unique in their chemical structure which lie in-between them, it is expected that these materials will provide interesting properties which cannot be offered by the conventional poly-

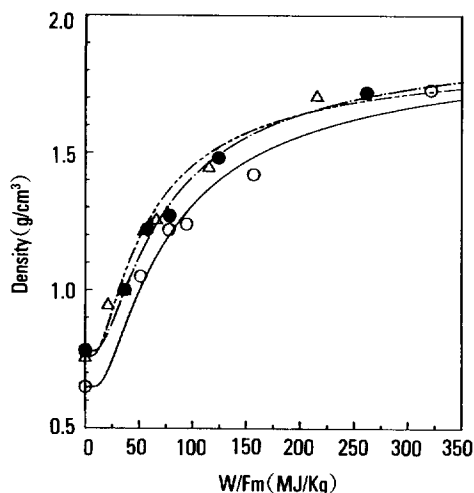


Fig. 2. Density of organosilicon plasma polymer as a function of W/Fm. (○) TMS, (●) HMDSIZ, (△) HMDSIO. The lines represent the relationship of eq 4.

mers or inorganics.

Fig. 2 shows the density change of organosilicon plasma polymer as a function of W/Fm. By adjusting the value of W/Fm only in the 20~350 MJ/Kg range, the density of plasma polymer changed dramatically in the range of 1.0~1.8 g/cm<sup>3</sup> for all the three monomers. Plasma polymer prepared at higher than 350 MJ/Kg was extremely dense to be scraped out as a visible film or particle so its density value could not be determined by the gradient column method. On the other hand, the plasma polymer prepared at lower than 20 MJ/Kg was a sticky liquid-like film, thus it was also difficult to measure the density by the gradient column methods. Thus, the density of plasma polymer at these two ranges could only be calculated by the thickness and weight gain on substrate. In fact, it was found that the density of plasma polymer at higher than 350 MJ/Kg approached 2.0 g/cm<sup>3</sup> and that of plasma polymer formed at lower than 20 MJ/Kg was less than 1.0 g/cm<sup>3</sup>. However, the density of plasma polymer obtained by this thickness-weight method is not included in Fig. 2 due to its insufficient accuracy compared to the gradient co-

lumn method. In the Fig's 4~6 of Part I<sup>3</sup>, we already observed that the chemical structure of organosilicon plasma polymer gradually changed from the polymer-like structure to the inorganic covalent structure with increasing W/Fm (almost the same range of W/Fm as for Fig. 2). It seems that the density change shown in Fig. 2 is closely related to this structure change since the density of polydimethylsiloxane<sup>7</sup> (organosilicon "polymer") is 0.98 g/cm<sup>3</sup>, that of inorganic thin films (e. g. silicon carbide, silicon nitride, silicon dioxide)<sup>7</sup> is higher than 2.0 g/cm<sup>3</sup>, and the range of density change shown in Fig. 2 is just between these two values controlled by W/Fm. From the regression analysis of data points, it was found that the density of organosilicon plasma polymer was empirically related to the input energy level (W/Fm) as eq 4 (visualized as the lines in Fig. 2).

$$d = d_0 + c_1 \exp(-c_2/(W/Fm)) \quad (4)$$

where,  $d$  is the density of plasma polymer (g/cm<sup>3</sup>),  $d_0$  is the density of monomer (0.65 g/cm<sup>3</sup> for TMS, 0.78 g/cm<sup>3</sup> for HMDSIZ, and 0.76 g/cm<sup>3</sup> for HMDSIO),  $c_1$  is a constant in the unit of g/cm<sup>3</sup> (1.26 for TMS, 1.17 for HMDSIZ, and 1.12 for HMDSIO), and  $c_2$  is another constant in the unit of MJ/Kg (64.9 for TMS, 62.0 for HMDSIZ, and 48.3 for HMDSIO). At present, eq 4 is only empirical, however it seems to describe the density change much quantitatively in terms of W/Fm and is possibly related to the activation growth nature of plasma polymerization<sup>3</sup> through the exponential term describing an activated reaction driven by the input energy level W/Fm (see Part III).<sup>8</sup>

Fig. 3 shows the contact angle ( $\theta_w$ ) change of plasma polymer as a function of plasma polymerization time. Very short deposition time (approximately 4 sec) seems to be sufficient to make the substrate surface to be homogeneously coated by plasma polymer after then the value of  $\theta_w$  is well stabilized. However, as can be expected from the significant change in the chemical structure,<sup>3</sup> the contact angle values were strongly affected by the input energy level (W/Fm) of plasma reaction. Ta-

**Table 1.** Surface Tension Values of Test Liquids<sup>5</sup>

Test Liquid	$\gamma_s^d$ (dyne/cm)	$\gamma_s^p$ (dyne/cm)	$\gamma_s$ (dyne/cm)
Water	21.8	51.0	72.8
Methylene Iodide	48.5	2.3	50.8

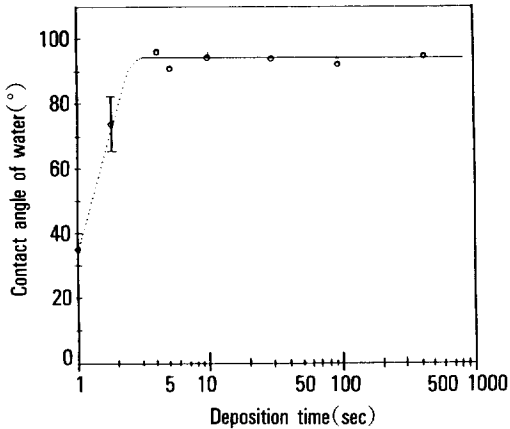


**Fig. 3.** Water contact angle( $\theta_w$ ) of organosilicon plasma polymer as a function of deposition time on the glass substrate.(Plasma polymer of HMDSIZ at W= 50 watt, Fm=24.1 mg/min, P<sub>0</sub>= 80 millitorr, W/Fm= 124.4 MJ/Kg ; 0.57  $\mu$ m thickness after 20 min deposition ; closed circle represents  $\theta_w$  of bare substrate)

Table 2 summarizes the measured contact angles  $\theta_w$  and  $\theta_i$ , and also the calculated surface free energy and its components( $\gamma_s$ ,  $\gamma_s^d$ ,  $\gamma_s^p$ ) of plasma polymer. From this table, it is apparent that the organosilicon plasma polymers are very hydrophobic since the polar component of surface energy( $\gamma_s^p$ ) is an order of magnitude smaller than the dispersion component of surface energy( $\gamma_s^d$ ). According to Wrobel,<sup>9</sup>  $\gamma_s^d$  is related to the chemical structure of material as eq 5.

$$\gamma_s^d = \frac{\pi N^2 \alpha^2 I^2}{8 r^2} \quad (5)$$

where, N is the number of volume elements per unit volume,  $\alpha$  is the polarizability, I is the ionization potential, and r is the average distance bet-

ween the volume elements. Since the density of plasma polymer increases significantly with W/Fm (shown in Fig. 2),  $\gamma_s^d$  is expected to increase with W/Fm by means of the increased N and decreased r in eq 5. In fact, such variations of  $\gamma_s^d$  are well identified in Table 2 for all the three organosilicon monomers. Some differences of  $\gamma_s^d$  due to the chemical structure of monomer can be found in the W/Fm range of less than 50 MJ/Kg. At this low input energy region,  $\gamma_s^d$  of HMDSIO plasma polymer is significantly lower than those of TMS and HMDSIZ. The polar component of surface energy  $\gamma_s^p$  shown in the sixth column of Table 2 also seems to increase with W/Fm although their absolute value is very low( $< 3 \text{ erg/cm}^2$ ). Generally, the plasma polymer retains an appreciable amount of trapped radical due to the activation growth nature of polymerization mechanism, thus the polar chemical bonds are formed through the post-plasma reaction of trapped radical with atmospheric oxygen or moisture.<sup>2</sup> Considering the effect of W/Fm on the activation reaction,<sup>3</sup> the concentration of trapped radical is expected to increase with W/Fm, as was indirectly confirmed by the steady increase of O/Si ratio with W/Fm as shown in Part I of this study.<sup>3</sup> Consequently, the plasma polymer prepared at the higher W/Fm is expected to show relatively higher value of  $\gamma_s^p$  if it received same aging (for example, one day aging in ambient air for Table 2). The effect of aging time on the surface energy components of HMDSIZ plasma polymer is shown in Fig. 4. It shows that  $\gamma_s^p$  of higher W/Fm plasma polymer is not much different from that of lower W/Fm plasma polymer immediately after deposition, however, it increases steadily to the significantly higher equilibrium value with continued aging. In a sense of the technological application of plasma polymer, such a long-term aging phenomena is never desirable since it causes the instability of surface property. Table 3 shows the improvement of aging property by the post-plasma thermal treatment. It is apparent from this table that the thermal treatment in air accelerates the aging phenomena, on the other hand, thermal

**Table 2.** Surface Free Energy of Organosilicon Plasma Polymer

Plasma Polymer	W/Fm (MJ/Kg)	$\theta_w$ (°)	$\theta_i$ (°)	$\gamma_s^d$ (erg/cm <sup>2</sup> )	$\gamma_s^p$ (erg/cm <sup>2</sup> )	$\gamma_s$ (erg/cm <sup>2</sup> )
TMS	18.1	103.6	62.5	27.3	0.2	27.5
	30.2	101.5	59.2	29.1	0.3	29.4
	31.4	97.5	58.6	28.6	0.9	29.5
	77.7	98.7	55.2	31.2	0.5	31.7
	94.2	95.2	51.1	33.0	0.8	33.8
	157.1	95.2	45.0	37.0	0.4	37.4
	321.3	92.7	43.1	37.5	0.7	38.2
	591.8	90.3	40.0	38.7	1.0	39.7
HMDSIZ	12.3	98.5	56.8	30.0	0.6	30.6
	20.5	97.1	60.0	27.5	1.1	28.6
	26.1	98.9	60.3	27.7	0.8	28.5
	57.6	95.7	56.4	29.6	1.1	30.7
	78.4	95.7	55.8	30.0	1.0	31.0
	124.4	93.7	55.6	29.6	1.5	31.1
	261.4	91.3	49.1	33.3	1.5	34.8
	480.7	85.7	43.8	35.2	2.6	37.8
HMDSIO	12.6	106.2	70.4	22.5	0.3	22.8
	21.0	104.7	69.6	22.8	0.5	23.3
	23.0	103.8	68.5	23.3	0.5	23.8
	54.3	103.0	64.5	25.8	0.4	26.2
	66.1	99.6	61.3	27.2	0.7	27.9
	115.3	96.3	57.4	29.1	1.0	30.1
	215.3	92.1	51.9	31.7	1.5	33.2
	417.2	86.8	43.1	35.9	2.2	38.1

\* Contact angles of water( $\theta_w$ ) and methylene iodide( $\theta_i$ ) were measured at the next day of plasma polymer deposition. The standard deviations of these contact angle measurement were generally less than 2°, which are not shown in this table for simplicity.

treatment in vacuum deactivates the aging possibly by the recombination of trapped radicals.

Fig. 5 shows the change of refractive indices according to W/Fm of plasma polymerization. The refractive indices of TMS and HMDSIZ plasma polymers increase steadily with the values of W/Fm in accordance with the enhanced inorganic character of the higher W/Fm plasma polymer<sup>3</sup>. In contrast, those of HMDSIO plasma polymers increase initially with W/Fm, however they decrease significantly at much higher W/Fm level. Such behavior is thought to result from the low refractive

index value of inorganic SiO<sub>2</sub>-like structure formed at this conditions.<sup>3</sup> Anyhow, Fig. 5 readily suggests that the tailoring of thin film material with well controlled refractive index is possible by the simple change of W/Fm value. Since the refractive index of material increases partially with the density of material, the results shown in Fig. 5 are thought to be the natural consequence of density change which originate from the activation growth nature of plasma polymerization.

Fig. 6 shows the internal stress in the HMDSIO plasma polymer as a function of W/Fm. According

**Table 3.** Effect of Thermal Treatments on the Surface Energy Components of HMDSIZ Plasma Polymer

W/Fm (MJ/Kg)	Treatment Method	$\theta_w$ ( $^\circ$ )* <sup>4</sup>	$\theta_i$ ( $^\circ$ )* <sup>4</sup>	$\gamma_s^d$ (erg/cm <sup>2</sup> )	$\gamma_s^p$ (erg/cm <sup>2</sup> )	Aging Effect
20.5	none	97.0	61.0	26.8	1.2	yes
	oven* <sup>1</sup>	98.2	62.7	26.0	1.1	no
	vacuum* <sup>2</sup>	100.2	62.0	26.9	0.6	no
	substrate* <sup>3</sup>	98.4	61.3	27.0	0.9	yes
124.4	none	94.1	54.8	30.3	1.3	yes
	oven* <sup>1</sup>	80.1	49.5	30.2	5.7	no
	vacuum* <sup>2</sup>	101.6	57.6	30.2	0.2	no
	substrate* <sup>3</sup>	91.5	50.8	32.3	1.6	yes

\*<sup>1</sup> : Thermal treatment in oven, 200°C, 30 min immediately after deposition.

\*<sup>2</sup> : Thermal treatment in plasma reactor after evacuation down to 10<sup>-3</sup> torr without opening to ambient air, 190°C, 30 min.

\*<sup>3</sup> : Substrate was constantly heated to 190°C during plasma polymerization.

\*<sup>4</sup> : Contact angles of water( $\theta_w$ ) and methylene iodide( $\theta_i$ ) were measured at the next day of plasma polymer deposition.

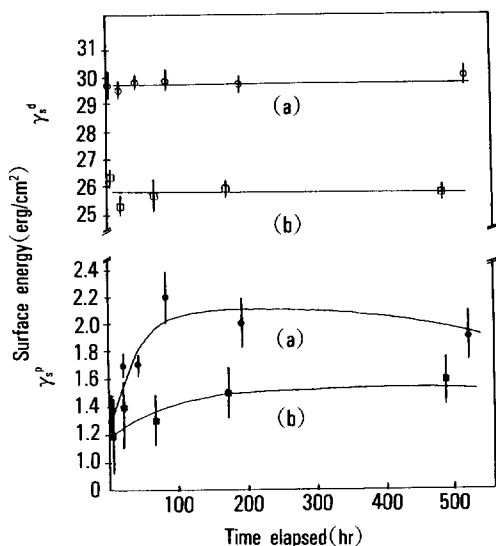


**Fig. 4.** Effect of W/Fm on the aging properties of surface energy components  $\gamma_s^d$  and  $\gamma_s^p$ : (a) HMDSIZ plasma polymer at W=50 watt, Fm=24.1 mg/min, P<sub>0</sub>=80 millitorr, W/Fm=124.4 MJ/Kg, (b) HMDSIZ plasma polymer at W=50 watt, Fm=146.2 mg/min, P<sub>0</sub>=200 millitorr, W/Fm=21.0 MJ/Kg.

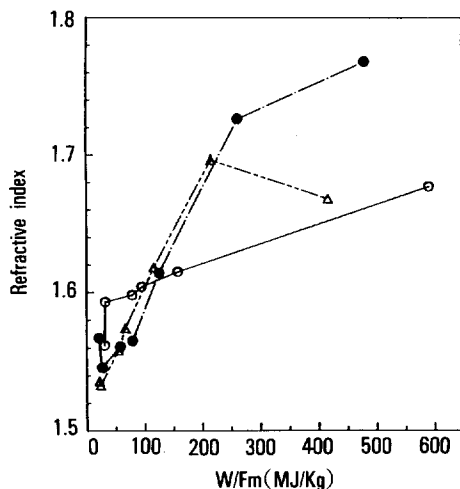


**Fig. 5.** Effect of W/Fm on the refractive index of plasma polymer. (O) TMS, (●) HMDSIZ, (Δ) HMD-SIO.

tics during the recombination reaction between the reactive species diffused from the vapor phase and the reactive sites in the surface of plasma polymer. Considering the activation growth reaction mechanism,<sup>2,3,6</sup> the magnitude of this stress is expected to increase with increasing W/Fm since it increases the degree of activation of molecular bonds per

to the work of Yasuda,<sup>6</sup> such internal stresses are thought to originate from the wedging characteris-

molecule.

Fig. 7 shows the TGA thermogram of TMS plasma polymer under nitrogen and oxygen atmosphere. Elevation of temperature under oxygen is thought to promote the oxidation of trapped radicals and the highly reactive hydrosilyl groups of plasma polymer, thus, weight increase of 4~5% of initial polymer weight is clearly observed before the thermal degradation of structure occurs, on the other hand, no significant weight gain was obser-

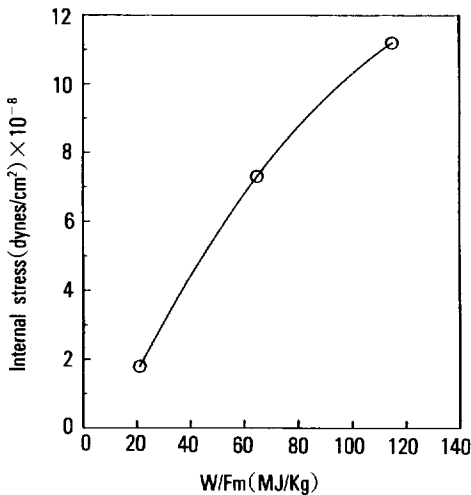


Fig. 6. Internal stress of HMDSIO plasma polymer film as a function of W/Fm.

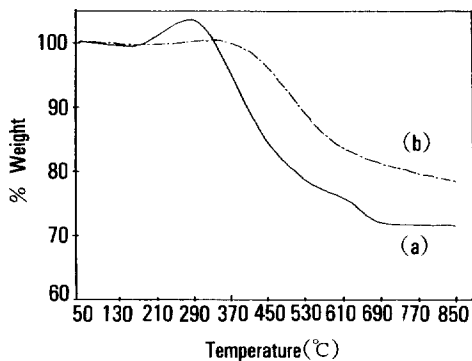


Fig. 7. TGA thermogram of TMS plasma polymer under (a) oxygen and (b) nitrogen atmosphere.(plasma polymer at W=30 watt, Fm=19.1 mg/min, P<sub>0</sub>=80 millitorr, W/Fm=94.2 MJ/Kg).

ved under nitrogen. Similar weight gain behavior was observed in the TGA thermogram of HMDSIZ and HMDSIO under air. Since the chemical structure of plasma polymer was significantly altered by W/Fm,<sup>3</sup> it is expected that the thermal stability will also be changed as such. TGA/DTA thermogram of HMDSIZ plasma polymers at two W/Fm shown in Fig. 8 visualizes well this fact.

According to the dense chemical structure(Part I)<sup>3</sup> and increased polar character( $\gamma_s^p$ ) at higher W/Fm, the dielectric constant( $\epsilon$ ) and dissipation factor (D) of plasma polymer also increases significantly with W/Fm as shown in Fig. 9. Fig. 10 shows the comparison of the DC conduction properties of HMDSIO MIM cells prepared from three different W/Fm condition in the coordinates of current density(j : amp/cm<sup>2</sup>) versus electric field (E : V/cm). These cells show ohmic conductivity up to the electric field designated as arrows in the figure, then non-ohmic conductivity(slope higher than 2) is observed at higher field. We find two distinct characteristics in this plot, namely, specific conductivity(j/E) of plasma polymer increased with W/Fm and the transition field from ohmic to non-ohmic was lowered with increasing W/Fm. At present, the mechanism of non-ohmic conductivity in a plasma polymer film is not well understood,<sup>2,10~13</sup> however, Poole-Frenkel mechanism<sup>10</sup>

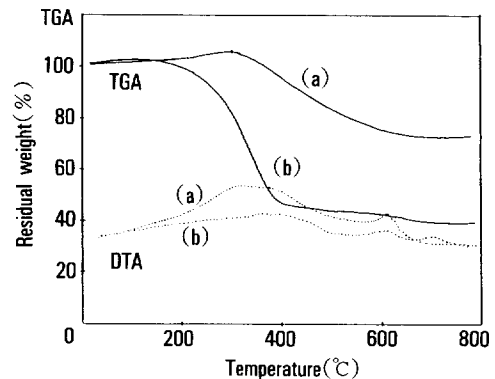


Fig. 8. Thermal properties of HMDSIZ plasma polymers prepared at W/Fm condition of (a) 78.4 MJ/Kg and (b) 12.3 MJ/Kg.



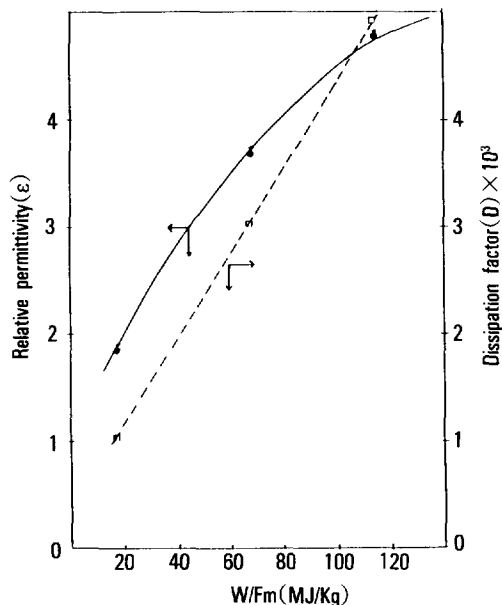


Fig. 9. Relative permittivity and dissipation factor of HMDSIO plasma polymer as a function of W/Fm.

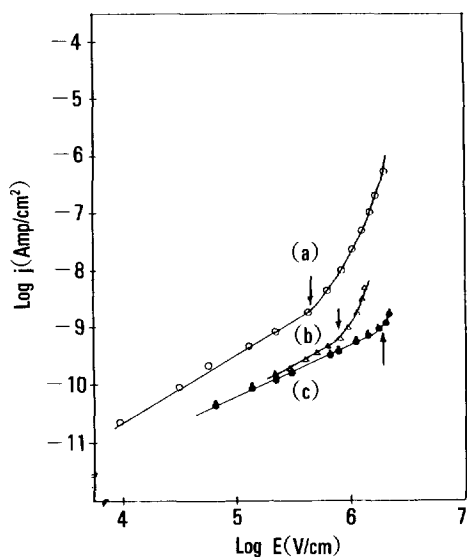


Fig. 10. DC conducting properties of thin (approximately 4000 Å) HMDSIO plasma polymers prepared at W/Fm conditions of (a) 115.3 MJ/Kg, (b) 66.1 MJ/Kg, (c) 21.0 MJ/Kg.

which describes the controlled activation of carrier detrapping process by the applied electric field is thought to play a major role in the non-ohmic conductivity. According to Szeto,<sup>13</sup> the electric conduction by Schottky mechanism cannot be excluded especially in the aged samples of plasma polymer due to the high density of surface states. Anyhow, the plasma polymers prepared at the higher W/Fm are characterized to be more dense in a chemical structure, to contain more local traps such as the trapped radicals and its oxidized product including the surface states, thus, are possibly thought to show the higher specific conductivity and lowered transition field.

### CONCLUSION

The physical properties of plasma polymer were found to be controlled by the input energy level W/Fm in good correlation with the chemical structure change, which could be explained by the activation growth nature of plasma polymerization. Actually, it was found that the plasma polymers possessing the higher density, surface energy, refractive index, internal stress, thermal stability, dielectric constant, dissipation factor, and electric conductivity were obtained at the higher W/Fm condition.

### REFERENCES

1. see References 3~16 of Part I.<sup>3</sup>
2. H. Yasuda, "Plasma Polymerization", Academic Press, New York, 1985.
3. S. Y. Park, N. Kim, U. Y. Kim, S. I. Hong, and H. Sasabe, *Polymer (Korea)*, **16**(1), (1992). (Part I of this series of paper).
4. D. K. Owens and R. C. Wendt, *J. Appl. Polym. Sci.*, **13**, 1741(1969).
5. D. K. Kaelble and E. H. Cirilin, *J. Polym. Sci. Pt. A2*, **9**, 363(1971).
6. H. Yasuda, T. Hirotsu, and H. G. Olf, *J. Appl. Polym. Sci.*, **21**, 3179(1977).
7. J. Mort and F. Jansen(eds), "Plasma Deposited

- Thin Films", CRC Press Inc., Florida, 1986.
8. S. Y. Park, N. Kim, U. Y. Kim, S. I. Hong, and H. Sasabe, *Polymer (Korea)*, **16**(3), in press (1992). (Part III of this series of paper).
  9. A. M. Wrobel in "Physicochemical Aspects of Polymer Surfaces, Vol. I", K. L. Mittal(eds), Plenum Press, New York, 1983.
  10. J. Tyczkowski, G. Czeremuskin, and M. Kryszewski, *Phys. Stat. Sol.*, **A72**, 751(1982).
  11. S. Morita, T. Mizutani, and M. Ieda, *Japan. J. Appl. Phys.*, **10**, 1275(1971).
  12. J. Tyczkowski and M. Kryszewski, *Phys. Stat. Sol.*, **A78**, 259(1983).
  13. R. Szeto and D. W. Hess, *Thin Solid Films*, **78**, 125(1981).